Journal of Hazardous Materials 199–200 (2012) 426–432

Contents lists available at SciVerse ScienceDirect

Journal of Hazardous Materials

journal homepage: www.elsevier.com/locate/jhazmat

Effects of the interaction of TiO_2 nanoparticles with bisphenol A on their physicochemical properties and in vitro toxicity

Dan Zheng[a], Nan Wang[b], Xinmei Wang[a], Ying Tang[c], Lihua Zhu[b], Zheng Huang[a,*], Heqing Tang[b], Yun Shi[a], Yating Wu[a], Meng Zhang[a], Bin Lu[a,**]

[a] MOE Key Laboratory of Environment and Health, School of Public Health, Tongji Medical College, Huazhong University of Science and Technology, #13 Hangkong Road, Wuhan, Hubei 430030, China
[b] College of Chemistry and Chemical Engineering, Huazhong University of Science and Technology, # 1037 Luoyu Road, Wuhan, Hubei 430074, China
[c] Naval Medical Research Institute, #880 Xiangying Road, Shanghai 200433, China

ARTICLE INFO

Article history:
Received 21 June 2011
Received in revised form
10 November 2011
Accepted 10 November 2011
Available online 20 November 2011

Keywords:
Titanium dioxide nanoparticles
Bisphenol A
Physicochemical characters
Synergistic toxicity
L-02 human hepatocytes

ABSTRACT

In this paper we evaluated the effects of the interaction of TiO_2 nanoparticles (nano-TiO_2) with bisphenol A (BPA) on their physicochemical properties and in vitro toxicity in human embryo L-02 hepatocytes. Different concentrations of BPA (0, 0.1, 1, 10 μmol/L) and nano-TiO_2 (0, 0.1, 1, 10 mg/L) were mixed to analyze the size distribution, zeta potential, adsorption capacity and uptake of nano-TiO_2, and the toxicity of nano-TiO_2 and BPA in L-02 cells. The addition of BPA to nano-TiO_2 dispersions increased the aggregation level and zeta potential of nano-TiO_2 in all media. Nano-TiO_2 had a similar adsorption capacity in different media, although a higher aggregation level was observed in cell culture medium. Nano-TiO_2, with or without BPA, could enter L-02 cells after 24 h exposure. Nano-TiO_2 alone did not induce significant DNA and chromosome damage, but the mixture of nano-TiO_2 and BPA increased toxicity via increasing oxidative stress, DNA double strand breaks and micronuclei formation. The aggregated nano-TiO_2 can enrich BPA effectively. The BPA-bound nano-TiO_2 are proven to be uptaken into nuclei of exposed cells, which may increase intracellular BPA and nano-TiO_2 levels and thus lead to synergistic toxicity. However only small synergic effects were observed at the concentrations of BPA and nano-TiO_2 used in this study.

1. Introduction

Titanium dioxide nanoparticles (nano-TiO_2) have been widely used as additives in cosmetics, pharmaceuticals, food colorants, sunscreens and coatings for self-cleaning windows. Nano-TiO_2 may react with a wide range of organic and biological molecules and then exhibit toxic effects in various cell lines, with or without photoactivation [1–3]. Several physicochemical characteristics, such as particle shape and size, surface area, agglomeration state, surface potential (zeta-potential) and surface chemistry are reported to be connected with the toxicity of nanoparticles [4]. Furthermore, these properties are dependent on environmental conditions. Particle concentrations, pH, the presence of electrolytes and other chemicals can influence the agglomeration, size distribution, zeta potential and stability of colloidal nano-TiO_2 [5,6]. It was reported that at higher concentrations, nano-TiO_2 showed increased agglomeration. Agglomeration levels of nano-TiO_2 in water and in cell culture medium were quite different [7].

Extensive usage of nano-TiO_2 increases the risk of combined exposure of nano-TiO_2 with other environmental pollutants. Bisphenol A (4,4-isopropylidine diphenol, BPA) is a monomer widely used for the production of polycarbonate plastics and epoxy resins, such as baby bottles, foodstuff containers and dental sealants. Regular consumption of cold beverages from polycarbonate bottles is associated with a substantial increase in urinary BPA concentrations [8]. BPA is an environmental estrogen disruptor that can cause adverse health effects on human beings by affecting growth, development, and reproduction. A daily exposure dose of 50 μg/kg body weight/day was stated to be safe for humans by the U.S. Food and Drug Administration and the U.S. Environmental

Abbreviations: Nano-TiO_2, titanium dioxide nanoparticles; BPA, bisphenol A; DMEM, Dulbecco's minimum essential eagle's medium; TEM, transmission electron microscopy; FT-IR, Fourier transform infrared spectrophotometer; DCFH-DA, 2,7-dichlorofluorescin diacetate; MN, micronucleus; LOQ, limit of quantification; LOD, limit of detection; MDA, malonaldehyde; ROS, reactive oxygen species; OTM, The Olive tail moment.

* Corresponding author.
** Corresponding author. Tel.: +86 27 83691809; fax: +86 27 83657765.
E-mail addresses: zhengdan@mails.tjmu.edu.cn (D. Zheng), wnanhust@yahoo.com.cn (N. Wang), wangzizi33@Tom.Com (X. Wang), maotou01@163.com (Y. Tang), lhzhu63@yahoo.com.cn (L. Zhu), huangzhg@mails.tjmu.edu.cn (Z. Huang), hqtang62@yahoo.com.cn (H. Tang), yunshi31@163.com (Y. Shi), 15095023@qq.com (Y. Wu), zm20080102@126.com (M. Zhang), lubin@mails.tjmu.edu.cn (B. Lu).

0304-3894/$ – see front matter © 2011 Elsevier B.V. All rights reserved.
doi:10.1016/j.jhazmat.2011.11.040

Protection Agency in the 1980s. Several in vivo and in vitro studies reported that significant adverse effects were observed at concentrations well below this predicted safe dose. Meanwhile other studies showed that no significant adverse effects were observed on rats at concentrations higher (200 μg/kg/day) than this predicted safe dose [9,10]. The extensive use of both BPA and nano-TiO_2 causes the serious possibility that BPA can interact easily with nano-TiO_2 in the environment. For example, the nano-TiO_2 photocatalytic degradation of BPA may result in an increased exposure risk of combined nano-TiO_2 and BPA if the degradation is not fully complete. The interaction may influence the agglomeration, colloidal stability and adsorption capacity of nano-TiO_2, which could affect adsorption, distribution, fate, intracellular exposure level and toxicity of both BPA and nano-TiO_2. According to the best of our knowledge, however, no study that focused on the interaction of nano-TiO_2 and BPA was reported.

The mixing of different compounds may induce unexpected toxic effects, even if the toxicities of the individual compounds are well known. The complexity of mixture toxicity lies in the potential for interaction between the mix constituents [11]. In our previous study, trace nano-TiO_2 that has no significant toxicity to human embryo hepatic L-02 cells enhanced the toxicity of trace p,p′-DDT synergistically. The effective adsorption of p,p′-DDT by nano-TiO_2 may contribute to this increase of toxicity [12]. Interactions of nanoparticles with organic chemicals were reported to affect physicochemical properties and adsorption of nanoparticles [13,14]. Therefore, exceptional physicochemical properties, adsorption kinetics and distribution of nano-TiO_2 should be considered together with the in vitro toxicity of nano-TiO_2 and BPA mixture at the same time.

In this study, effects of the interaction of nano-TiO_2 with BPA on the physicochemical properties (including particle size, zeta potential and adsorption kinetics), uptake of nano-TiO_2 by L-02 cells and in vitro toxicity of nano-TiO_2 and BPA were studied synchronously. The liver is the major organ to metabolite BPA [9], and the location in which nano-TiO_2 accumulates mainly following either oral administration or intravenous administration [15,16]. Therefore, we used human embryo hepatic L-02 cell as a model to study the uptake and toxicity of BPA and nano-TiO_2 exposure. Furthermore, nano-TiO_2 induced oxidative stress, DNA damage and micronuclei formation [1–3]. BPA produced oxidative stress and DNA damage in cultured cells and in rodents [9,17,18]. For these reasons, we used intracellular oxidative stress, DNA breaks, chromosome damage and cell viability as indexes to evaluate the toxicity of nano-TiO_2 and BPA exposure in L-02 cells.

2. Materials and methods

2.1. Nano-TiO_2 particle

Nano-TiO_2 (Degussa P25) was obtained from Degussa (Hanau, Germany). The crystalline anatase/rutile ratio is 8:2 with a primary particle diameter of approximately 25–50 nm (Fig. S1, supporting material) and BET surface area of 50 m^2/g. Nano-TiO_2 was sterilized in an autoclave and freshly suspended in distilled water immediately before use. Stock solution of BPA (20 mmol/L) was prepared in DMSO and stored at 4 °C.

2.2. Dispersion stability of nano-TiO_2

Size distribution and zeta potential of autoclaved nano-TiO_2, with or without BPA in distilled water, 0.2 g/L $CaCl_2$ solution or serum-free Dulbecco's minimum essential Eagle's medium (DMEM, containing 100 units/mL penicillin G and 100 μg/mL streptomycin, ph 7.7) were measured by dynamic light scattering using Zeta Potential & Photon Correlation Spectroscopy (Beckman Coulter, USA). Different concentrations of BPA and autoclaved nano-TiO_2 were mixed, vortexed for 2 min, ultrasonicated for 10 min, and then measured immediately. Time-dependent changes (0–60 min) in dispersion stability were analyzed in the mixture of 10 μmol/L BPA and 10 mg/L nano-TiO_2.

2.3. Uptake of nano-TiO_2 by L-02 cells

After L-02 cells were exposed to 10 mg/L nano-TiO_2 alone, 10 mg/L nano-TiO_2 and 10 μmol/L BPA for 24 h, the cells were collected, washed and fixed in 2.5% glutaraldehyde, post-fixed with OsO_4 and dehydrated in graded concentrations of ethanol and then embedded in Eponate-12 overnight. Ultra-thin sections were cut (80 nm), counterstained with lead citrate and uranyl acetate, and then observed with Tecnai G2 20 TWIN transmission electron microscopy (Fei, The Netherlands) at 200 kV.

2.4. Adsorption kinetics

Nano-TiO_2 suspension (10 mg/L) was mixed with 10 μmol/L BPA solutions (in distilled water, 0.2 g/L $CaCl_2$ or serum free DMEM at pH 7.7). The solutions were sealed and stirred at room temperature. At different intervals, samples were taken out. The supernatants were used for analysis after the solid particles were precipitated. BPA solutions at different concentrations without nano-TiO_2 were used as references. To prevent photodegradation of BPA by nano-TiO_2, the samples were covered with aluminum foil during the entire adsorption test. BPA in the supernatants was determined by Waters 1512 HPLC system with a 2487 dual λ absorbance detector (Waters, USA) at 281 nm on a Waters Symmetry reversed-phase ODS column (5 μm, 150 mm × 4.6 mm i.d.). The mobile phase was water–acetonitrile 5:5 (v/v). The calibration graph for BPA was linear in the range from 0.1 to 10 μmol/L with R^2 = 0.9996. The limit of detection (a signal-to-noise ratio of 3) was 0.01 μmol/L. The limit of quantification (a signal-to-noise ratio of 10) was 0.1 μmol/L.

The binding of BPA to nano-TiO_2 was also detected on a Bruker VERTEX 70 Fourier transform infrared spectrophotometer (FT-IR) equipped with ATR accessory. Considering the detection sensitivity and requirements of FT-IR, high concentration of BPA (20 μmol/L) was mixed with high level (486.7 mg/L) of nano-TiO_2 in distilled water at pH 7.7 for 24 h. Then nano-TiO_2 was separated and washed 4 times with distilled water. After being precipitated, the samples were dried at 25 °C in a vacuum oven for 24 h prior to FT-IR analysis. Scans of the region between 500 and 4000 cm^{-1} were collected for each FT-IR spectrum.

2.5. Cell culture and treatment

A human embryo hepatic L-02 cell line was purchased from the China Center for Type Culture Collection (Wuhan University, China). L-02 cells were grown in DMEM containing 10% fetal bovine serum, 100 units/mL penicillin G and 100 μg/mL streptomycin at 37 °C in a humidified atmosphere containing 5% CO_2. Cells were seeded in 24-well plates at a density of 1×10^5 cells/well. After seeding for 24 h, the cells were washed and treated with a series of nano-TiO_2 (0, 1, 5, 10 mg/L) and/or BPA (0, 0.1, 1, 10 μmol/L), respectively, in DMEM without fetal bovine serum in the dark. As BPA was prepared in DMSO, control cells were treated with an equal volume of DMEM containing 0.1% DMSO.

2.6. Cell viability

Intracellular ATP level was used to determine the viability of exposed L-02 cells. In brief, following either 6, 12, or 24 h of exposure, DMEM medium was removed and 2% trichloroacetic acid was

applied to the L-02 cells to extract ATP. Then the sample was neutralized to pH 7.7 and the trichloroacetic acid was diluted to a final concentration of 0.1% or less by adding Tris–HCl buffer (0.1 mol/L, pH 9.0). ATP was measured according to the protocol of ENLITEN ATP Assay kit (Promaga, USA).

2.7. Intracellular oxidative stress

Intracellular reactive oxidative species (ROS) were measured by flow cytometry using 2,7-dichlorofluorescein diacetate (DCFH-DA) as a probe [19]. After 24 h exposure, L-02 cells were washed twice and mixed with 10 μmol/L DCFH-DA for 30 min at 37 °C in the dark. Fluorescent intensities were measured at 488 nm excitation, 525 nm emission using a FACS420 flow cytometer (Becton-Dickison, USA). Background fluorescence was subtracted from the measured values.

The levels of malonaldehyde (MDA) were determined following the method of Yagi [20] according to the protocol of a MDA assay kit (Jiancheng Bioeng Inst., Nanjing, China).

2.8. DNA damage

DNA double strand breaks were detected by neutral comet assay [21]. After 24 h exposure, 1×10^5 cells suspended in 100 μL 0.5% low melting agarose in PBS were spread on normal melting agarose-coated (1%) slides. The slides were covered with a coverslip and kept at 4 °C to solidify the low melting agarose. Thereafter, the coverslips were removed and the slides were transferred to a lysis buffer (2.5 mol/L NaCl, 100 mmol/L Na_2EDTA, 10 mmol/L Tris base, 1% Triton-X 100 and 10% DMSO) for 1 h at 4 °C. Slides were transferred to an electrophoresis cell containing 300 mmol/L sodium acetate and 100 mmol/L Tris–HCl, pH 8.5 for 20 min at 4 °C, then subjected to electrophoresis for 40 min at 25 V (240 mA). Subsequently, all slides were rinsed with Tris–HCl buffer (0.4 mol/L, pH 7.5), stained with ethidium bromide (10 μg/mL), and examined with an Olympus fluorescence microscope at 515–560 nm excitation and 590 nm emission. From each sample, 100 randomly selected cells were analyzed. The Olive tail moment (OTM) of each comet was calculated using CASP analysis software (Olive Tail Moment = percent of DNA in the tail × distance between the center of gravity of DNA in the tail and the center of gravity of DNA in the head).

2.9. Chromosome damage

The in vitro micronucleus (MN) assay was performed [22] to detect chromosome damage. After 24 h exposure, L-02 cells were washed twice with PBS. Cytochalasin B (final concentration 3 μg/mL) was added in fresh DMEM for another 24 h. Thereafter, cells were harvested and re-suspended in cold hypotonic solution (0.075 mol/L KCl) for 1 min, gently fixed in a methanol/acetic acid (3:1) solution twice, re-suspended in a small volume of methanol/acetic acid, and dropped onto clean slides. The slides were stained with Giemsa solution (10%) and analyzed using a light microscope (Olympus DP70). Micronuclei in 3000 binucleated cells with well-preserved cytoplasm were scored for each group.

2.10. Statistics

All physicochemical experiments were performed in triplicate. Cells experiments were performed in quadruplicate wells in three independent tests. The results of 12 individual values are presented as mean values and standard deviations. ANOVA and the Pearson correlation coefficient were carried out by SPSS (version 13.0). Significance was assessed at the 95% confidence level ($P < 0.05$) for all tests. In vitro interactions were analyzed using a response surface model (RSM) by Design expert software (version 7.1). *P*-values generated using RSM indicate additivity if $P \geq 0.05$, and synergy if $P < 0.05$ [11].

3. Results and discussion

3.1. Effects of nano-TiO_2 and BPA interactions on physicochemical properties of nano-TiO_2

Agglomeration and surface properties are important characteristics that affect distribution and toxicity of nanoparticles [4–7,14]. High absolute values of the zeta potentials ensure a stable suspension in media because of the strong electrostatic repulsion [5,7,14]. Nano-TiO_2 agglomerated more significantly in the cell medium than in distilled water. However the influence of different physiological media (PBS, HBSS, DMEM) on agglomeration and zeta potential of nano-TiO_2 were similar [7]. A negative zeta potential level (Table 1) indicated that nano-TiO_2 (Dugass P25, Fig. S1) used in this study was negative charge at pH 7.7. Ca^{2+} (0.2 g/L $CaCl_2$) is the highest concentration of cation in DMEM medium. Compared with distilled water, nano-TiO_2 had a higher agglomeration level and zeta potential in $CaCl_2$ and DMEM. However, nano-TiO_2 had a similar zeta potential and agglomeration level in $CaCl_2$ and DMEM, indicating that cations such as Ca^{2+} can combine with negatively charged nano-TiO_2 effectively by cation bridging to increase zeta potential. High zeta potential was optimal to form agglomerates in DMEM. Furthermore, a higher nano-TiO_2 concentration enhanced direct particle-to-particle interaction [7], which favored the formation of agglomerates (Table 1).

The addition of fetal bovine serum and human serum albumin to DMEM reduced the agglomeration and zeta potential of nano-TiO_2, possibly due to the effect of steric stabilization [7]. In this study, the addition of BPA in DMEM without fetal bovine serum increased zeta potential and agglomeration of nano-TiO_2 in a dose–response (Table 1) and time-dependent (Fig. 1) model in all media. A higher agglomeration level of nano-TiO_2 was observed in DMEM and $CaCl_2$ than in distilled water. The agglomeration level and zeta potential in DMEM were a little higher than in $CaCl_2$, but the differences were not significant (Table 1 and Fig. 1). The most significant changes on agglomeration and zeta potential were observed between 10 and 20 min after mixing (Fig. S2). These may due to the fact that BPA (pK_a about 9.7) was not markedly dissociated at pH 7.7. BPA can compete with anions such as OH^- around the surface of nano-TiO_2 to reduce the negative charges around nano-TiO_2 and enhance agglomeration. As the contact time and BPA level were increased, more and more BPA was bound onto the surface of nano-TiO_2. Therefore both zeta potential and agglomeration were increased with the increase of BPA concentration and binding time.

Size distribution and surface charge can modify the adsorption capacity of nano-TiO_2 [12,14,23]. Electrostatic interaction and ligand exchange were proposed for adsorption of natural organic materials onto mineral surfaces of nano-TiO_2 [14]. Moreover, ligand exchange was responsible for the binding of humic acid to nano-TiO_2 [12]. At pH 7.7, the binding capacity of nano-TiO_2 in water, $CaCl_2$ and DMEM media were similar (about 0.23 μmol BPA/g nano-TiO_2, Fig. 2), although nano-TiO_2 particles agglomerated more significantly in $CaCl_2$ and DMEM media (Table 1 and Fig. 1). Well-defined plateaus were observed after 4–5 h adsorption when the initial concentration of BPA was 10 μmol/L (Fig. 2). Agglomerated nano-TiO_2 in $CaCl_2$ or DMEM media had similar adsorption capacity compared with less agglomerated nano-TiO_2 in distilled water. Agglomeration did not affect adsorption capacity of nano-TiO_2. FT-IR spectra analysis showed that significant BPA spectra were observed on nano-TiO_2 surfaces, which further confirmed the effective adsorption of BPA by nano-TiO_2 in distilled water (Fig. 3). Because BPA did not ionize markedly at pH 7.7, the

Table 1
Average particle size and zeta potential of nano-TiO_2 and BPA mixture in different solutions ($n = 3$).

BPA (μmol/L)	Particle size[a]	nano-TiO_2 (mg/L)		Zeta potential	nano-TiO_2 (mg/L)	
	1	5	10	1	5	10
Water						
0	210.4 ± 7.29	275.5 ± 7.25	304.8 ± 8.18	−31.44 ± 1.38	−27.64 ± 1.14	−26.82 ± 1.38
0.1	220.1 ± 9.75	278.6 ± 7.30	313.27 ± 8.65	−31.43 ± 0.8	−27.55 ± 1.79	−26.33 ± 1.08
1	221.85 ± 7.00	320.5 ± 13.89	324 ± 8.23	−30.89 ± 1.61	−26.09 ± 1.37	−23.9 ± 1.08
10	224.7 ± 12.71	334.07 ± 3.99	337 ± 14.64	−30.63 ± 0.93	−25.85 ± 1.43	−23.27 ± 0.75
$CaCl_2$						
0	312.6 ± 6.99	414.9 ± 12.80	431.3 ± 2.72	−16.6 ± 1.06	−11.6 ± 0.56	−10.32 ± 0.87
0.1	371.3 ± 12.75	422.9 ± 7.24	448.4 ± 6.87	−4.205 ± 1.03	−11.18 ± 0.89	−9.06 ± 1.00
1	389.8 ± 4.11	448.7 ± 14.47	455.1 ± 6.01	−13.19 ± 0.81	−9.29 ± 1.18	−8.83 ± 0.72
10	404.9 ± 14.97	456.43 ± 13.49	478.3 ± 7.05	−12.985 ± 0.49	−7.2 ± 0.75	−6.92 ± 0.13
DMEM						
0	322.3 ± 8.84	367 ± 9.03	482.45 ± 3.06	−25.27 ± 0.94	−12.725 ± 0.66	−8.015 ± 0.27
0.1	341 ± 9.39	390.9 ± 2.25	496.8 ± 5.34	−16.94 ± 1.53	−11.685 ± 1.22	−7.49 ± 0.43
1	380.2 ± 0.92	402.9 ± 4.95	517.7 ± 6.69	−12.15 ± 1.03	−10.865 ± 0.47	−6.15 ± 0.35
10	457.4 ± 5.92	481.5 ± 8.67	561 ± 5.28	−11.555 ± 0.77	−8.07 ± 0.32	−5.94 ± 0.29

[a] Average size of the entire population from the dynamic light scattering experiments was used.

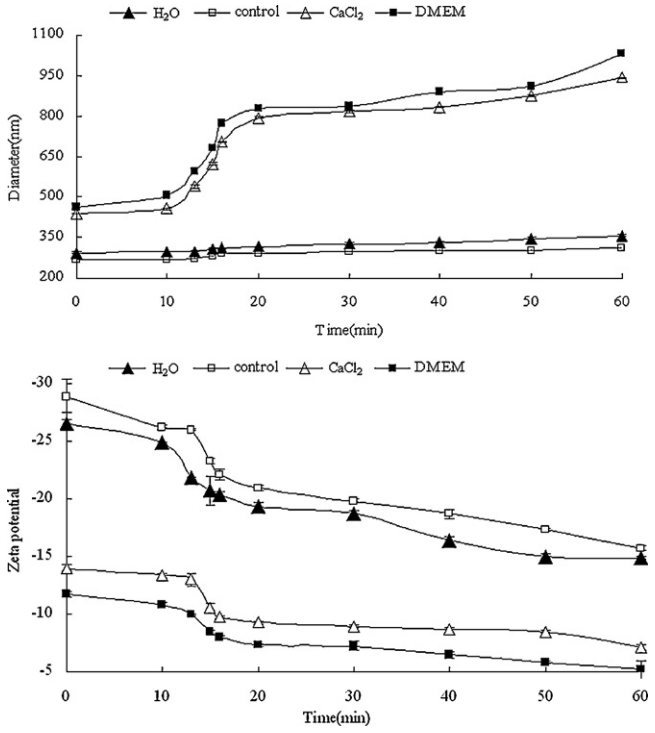

Fig. 1. Time-dependent size distribution and zeta potential of nano-TiO_2 in different media. Control: 10 mg/L nano-TiO_2 in distilled water; H_2O: 10 mg/L nano-TiO_2 in distilled water containing 10 μmol/L BPA; $CaCl_2$: 10 mg/L nano-TiO_2 in 0.2 g/L $CaCl_2$ solution containing 10 μmol/L BPA; DMEM: 10 mg/L nano-TiO_2 in DMEM containing 10 μmol/L BPA. Average size of the entire dynamic light scattering data was used.

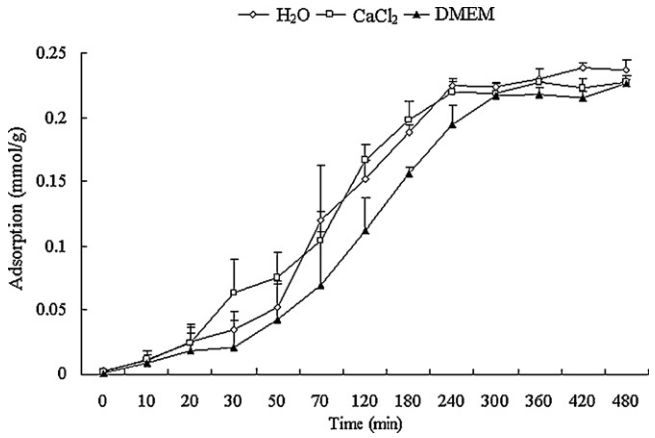

Fig. 2. Adsorption kinetics of 10 μmol/L BPA by 10 mg/L nano-TiO_2 in different media.

ligand exchange may be the main reason for the adsorption of BPA on the surfaces of nano-TiO_2.

3.2. Effects of nano-TiO_2 and BPA interaction on the uptake of nano-TiO_2 by L-02 cells

In vivo studies showed that nanoparticles can cross biological barriers without a specific transporter [24]. Nano-TiO_2 was distributed in cellular membranes, cytoplasm or loose-fitting phagosomes in several cell lines [2,3]. The uptake and toxicity of WC-Co nanoparticle was independent of the initial nanoparticle agglomeration state because agglomeration did not change the surface area of WC-Co nanoparticles dramatically. The relatively constant surface area did not change the reactivity and toxicity of the WC-Co nanoparticles significantly [25]. In this study, when BPA was mixed with nano-TiO_2, interactions of nano-TiO_2 with BPA increased agglomeration and zeta potential (Table 1 and Fig. 1). But both agglomerated BPA-bound nano-TiO_2 (Fig. 4B) or nano-TiO_2 alone (Fig. 4A) were visible within the cells and the nuclei after the L-02 cells were exposed to 10 mg/L nano-TiO_2 or 10 μmol/L BPA and 10 mg/L nano-TiO_2 for 24 h. The aggregated nano-TiO_2 can adsorb and enrich BPA effectively. The BPA-bound nano-TiO_2 are shown to be uptaken into nuclei of exposed L-02 cells, which will facilitate the movement of both BPA and nano-TiO_2 into exposed cells and increase the intracellular exposure level. Higher intracellular exposure levels may enhance toxicity of both BPA and

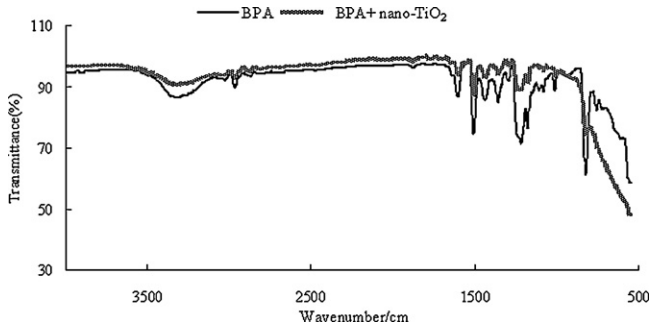

Fig. 3. FT-IR assay of BPA and nano-TiO_2 mixture in water after 24 h exposure. BPA concentration: 20 μmol/L BPA; nano-TiO_2 concentration: 486.7 mg/L.

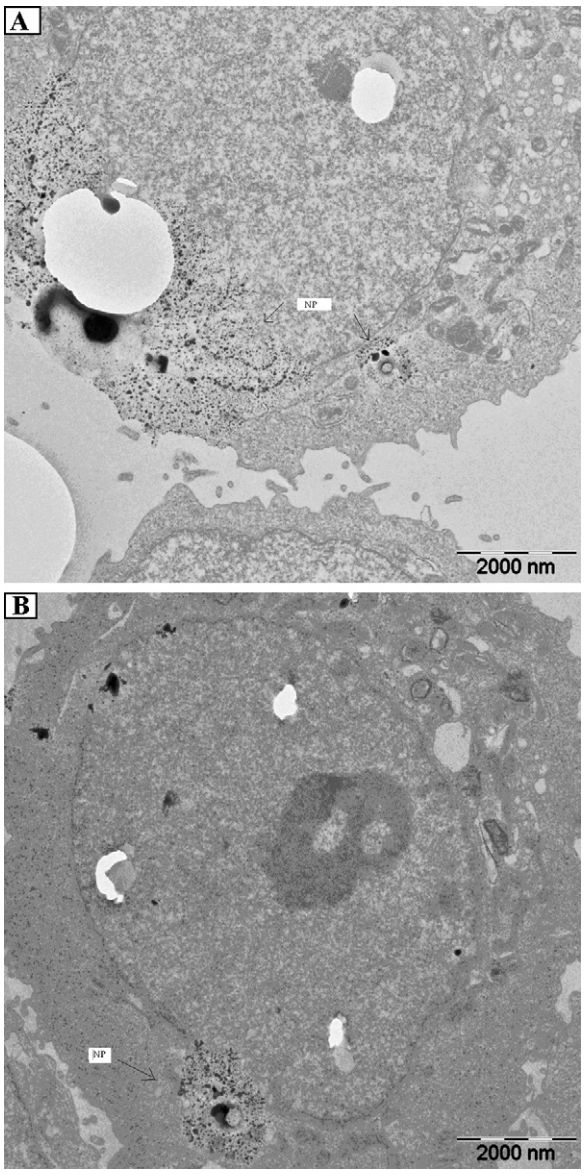

Fig. 4. SEM of L-02 cells exposed to 10 mg/L nano-TiO_2 alone (A) or 10 μmol/L BPA and 10 mg/L nano-TiO_2 (B) after 24 h exposure. Arrow: NP, nano-TiO_2 particles.

nano-TiO_2 after the cells are exposed to low levels of BPA and nano-TiO_2.

3.3. Toxicity of nano-TiO_2 and BPA mixture on L-02 cells

No significant toxicity of nano-TiO_2 (less than 1 mg/L) was observed in L-02 cells in our previous study [11]. Whereas BPA can promote cell viability at low doses it is cytotoxic at high doses [9,17]. Therefore, 0, 0.1, 1, 10 μmol/L BPA and 0, 1, 5, 10 mg/L nano-TiO_2 were used in this study. Different concentrations of BPA and nano-TiO_2, either used separately or as a mixture of the two chemicals, did not significantly affect ATP level and cell viability at three time points (6, 12, and 24 h). Because mitochondria are the site of ATP production, a lack of significant change in ATP levels indicates that concentrations of BPA and nano-TiO_2 used in this study did not induce noticeable mitochondrial dysfunctions. The similar cell viability of every group also indicated that there were no false positive responses due to cytotoxicity in the subsequent analysis (Table 2).

Either nano-TiO_2 or BPA alone can induce oxidative stress in vivo and in vitro. The ability of nano-TiO_2 to induce oxidative stress is correlated with the dose, chemical components and psychochemical characters of the nano-TiO_2. The most cytotoxic nano-TiO_2 was also the most effective at generating ROS [26,27]. Reaction of nano-TiO_2 with cell membranes and distribution of ultrafine particles inside mitochondria are potential mechanisms for the generation of ROS and oxidative stress [1–3]. BPA application induced ROS in Chang liver cells and in the liver and epididymal sperm of rats [28]. Urinary BPA concentrations were positively associated with MDA, 8-hydroxydeoxyguanosine and C-reactive protein levels in postmenopausal women [29]. When nano-TiO_2 and BPA were exposed together, BPA and nano-TiO_2 mixture had higher ROS levels and MDA levels than the corresponding groups treated with nano-TiO_2 or BPA alone (Table 3). Because $P < 0.05$ in an RSM model indicated synergy [11], synergistic responses for ROS ($F = 59.21$, $P < 0.0001$, Fig. S2A) and MDA ($F = 32.23$, $P < 0.0001$, Fig. S2B) generated by mixtures of BPA and nano-TiO_2 were observed. However, the net increases on ROS or MDA levels in BPA and nano-TiO_2 mixed groups were not much higher than in the corresponding groups treated with nano-TiO_2 or BPA alone. Therefore, the synergistic effects on ROS and MDA levels were not very strong at concentrations of BPA and nano-TiO_2 used in this study (Table 3). Furthermore, ROS levels changed more significantly than MDA levels, suggesting that cellular repair systems for oxidative damage were more capable of reducing ROS than of decreasing MDA levels after 24 h exposure to nano-TiO_2 and BPA. Effective uptake of agglomerated BPA-bound nano-TiO_2 increased intracellular BPA and nano-TiO_2 level after cells were exposed to low levels of BPA and nano-TiO_2, which may contribute to the increase in intracellular oxidative stress by the nano-TiO_2 and BPA mixture.

Intracellular BPA or nano-TiO_2 can attack DNA to induce DNA damage directly, or cause DNA damage indirectly via oxidative stress in cultured cells, rats and humans [1,9,12]. A neutral comet assay exclusively measures DNA double strand breaks [21]. In this study, nano-TiO_2 which did not induce DNA double strand breaks on its own, enhanced the capability of low levels of BPA to cause DNA double strand breaks (Table 4). According to an RSM model, a synergistic response for neutral OTM levels generated by a mixture of BPA and nano-TiO_2 was observed ($F = 213.93$, $P < 0.0001$, Fig. S2C). But the increases of OTM levels in cells treated by BPA and nano-TiO_2 mixtures were not very high compared with cells treated by nano-TiO_2 or BPA alone, which suggested that only a small magnitude synergism of OTM levels was generated at concentrations of BPA and nano-TiO_2 used in this study (Table 4). Pearson's analysis showed no significant correlation between neutral OTM levels and oxidative stress (between OTM and ROS generation, $r = 0.077$, $P = 0.605$; between OTM and MDA level, $r = 0.042$, $P = 0.779$). These

Table 2
Viability of L-02 cells exposed to different concentrations of nano-TiO_2 and BPA ($n = 6$).

BPA (μmol/L)	Nano-TiO_2 (mg/L)			
	0	1	5	10
6 h				
0	96.2 ± 5.1	97.3 ± 8.8	89.4 ± 3.2	91.5 ± 7.7
0.1	108.4 ± 8.1	92.3 ± 1.8	91.2 ± 5.5	88.4 ± 9.2
1	96.2 ± 7.4	91.1 ± 8.2	92.2 ± 2.7	92.8 ± 3.9
10	90.6 ± 5.5	97.1 ± 8.1	90.6 ± 4.3	88.3 ± 9.1
12 h				
0	92.6 ± 6.5	93.9 ± 2.7	92.2 ± 4.8	92.5 ± 3.4
0.1	103.1 ± 8.9	87.3 ± 2.3	90.4 ± 5.7	91.3 ± 6.4
1	101.5 ± 6.6	95.4 ± 5.4	90.5 ± 8.8	89.3 ± 6.2
10	89.5 ± 4.5	90.4 ± 6.2	91.1 ± 10.2	88.7 ± 5.4
24 h				
0	90.4 ± 5.2	91.1 ± 11.4	92.6 ± 7.2	89.6 ± 12.2
0.1	98.5 ± 9.2	90.8 ± 6.1	94.1 ± 9.3	90.5 ± 3.1
1	90.2 ± 8.1	94.4 ± 7.7	98.5 ± 12.3	91.4 ± 5.3
10	92.4 ± 5.5	92.8 ± 6.3	89.6 ± 10.1	88.7 ± 13.4

Table 3
Oxidative stress levels in L-02 cells exposed to different concentrations of nano-TiO_2 and BPA for 24 h.

Groups (n = 3)				
BPA(μmol/L)	Nano-TiO_2 (mg/L)			
	0	1	5	10
ROS (DCF fluorescence intensity)				
0	56.07 ± 1.60	57.87 ± 1.40	64.05 ± 2.27[a]	67.62 ± 1.41[a]
0.1	63.40 ± 1.89[a]	60.46 ± 1.74	67.46 ± 2.34[a]	75.60 ± 1.46[a,b,c]
1	68.22 ± 2.87[a]	72.62 ± 1.46[a,b]	75.56 ± 2.69[a,b,c]	85.15 ± 2.48[a,b,c]
10	73.33 ± 2.96[a]	77.58 ± 1.73[a,b]	86.24 ± 1.71[a,b,c]	94.74 ± 2.59[a,b,c]
MDA (μmol/L)				
0	0.42 ± 0.26	0.43 ± 0.22	0.47 ± 0.19	0.56 ± 0.06
0.1	0.43 ± 0.14	0.49 ± 0.23	0.58 ± 0.13	0.67 ± 0.14
1	0.59 ± 0.07	0.72 ± 0.24	0.77 ± 0.25[a]	0.80 ± 0.02[a]
10	0.74 ± 0.25	0.77 ± 0.30[a]	0.97 ± 0.40[a,b]	1.25 ± 0.64[a,b,c]

[a] P < 0.05 compared with control.
[b] P < 0.05 compared with correlated nano-TiO_2 groups.
[c] P < 0.05 compared with correlated BPA groups.

Table 4
Oliver tail moment (OTM) and micronucleus frequency in L-02 cells exposed to different concentrations of nano-TiO_2 and BPA for 24 h.

Groups (n = 3)				
BPA (μmol/L)	Nano-TiO_2 (mg/L)			
	0	1	5	10
OTM				
0	0.45 ± 0.57	0.46 ± 0.27	0.58 ± 1.01	0.63 ± 0.89
0.1	0.57 ± 0.44	0.67 ± 1.35	0.74 ± 0.81	0.84 ± 0.29
1	0.84 ± 0.18[a]	1.22 ± 1.14[a,b]	1.39 ± 0.65[a,b]	1.45 ± 0.15[a,b,c]
10	1.14 ± 0.17[a]	1.30 ± 0.19[a,b]	1.51 ± 0.94[a,b]	1.82 ± 0.37[a,b,c]
Micronucleus frequency				
0	2.33 ± 0.33	2.33 ± 0.33	2.00 ± 0.58	2.00 ± 0.05
0.1	3.00 ± 0.0.58	2.67 ± 0.88	3.00 ± 0.58	3.00 ± 0.58
1	3.67 ± 0.88	5.33 ± 1.20[a,b]	6.33 ± 0.88[a,b,c]	5.67 ± 0.88[a,b]
10	6.67 ± 0.33[a]	7.00 ± 0.58[a,b]	7.67 ± 0.88[a,b]	7.67 ± 0.67[a,b]

[a] P < 0.05 compared with control.
[b] P < 0.05 compared with correlated nano-TiO_2 groups.
[c] P < 0.05 compared with correlated BPA groups.

data indicated that oxidative stress was not the main reason to cause DNA double strand breaks in L-02 cells exposed to nano-TiO_2 and BPA. Because BPA-bounded nano-TiO_2 can enter the nuclei of exposed cells (Fig. 4), direct DNA damage caused by enriched intracellular nano-TiO_2 and BPA may be one reason to enhance DNA double strand breaks.

DNA double strand breaks and mitotic dysfunction are two main reasons for micronucleus formation. BPA or nano-TiO_2 alone can increase MN frequency. A dose-dependent increase in MN frequency was observed in many cell lines treated by BPA, either caused by DNA double strand breaks (clastogenic effects) or by mitotic dysfunction (aneugenic effects) [30]. A significant increase in MN formation was observed in SHE cells [26] treated with nano-TiO_2 for 12–72 h, which may be due to ROS and/or to the physical presence of these particles around the mitotic apparatus. Oxidative stress, DNA damage, and mitotic spindle dysfunction were potential factors involved in nano-TiO_2 induced MN formation [26]. In this study, nano-TiO_2, which did not induce MN formation on its own, enhanced the capability of BPA to induce MN formation (Table 4). An RSM model suggested that mixtures of BPA and nano-TiO_2 induced a synergistic response to MN frequency (F = 253.98, P < 0.0001, Fig. S2D). But the magnitude of synergistic effect was not very high at concentrations of BPA and nano-TiO_2 used in this study according to results of ANOVA tests (Table 4). Further analysis showed that no correlation between MN formation and DNA double strand breaks was observed (r = 0.026, P = 0.859). Nevertheless, positive correlations were observed in Pearson's analysis between MN formation and ROS levels (r = 0.559, P < 0.001), and between MN and MDA levels (r = 0.351, P = 0.015). BPA was reported to have aneuploidogenic properties in CHO-K1 cells [31]. When BPA and nano-TiO_2 were mixed together, BPA-bound nano-TiO_2 can enter the nuclei of exposure cells (Fig. 2). Therefore, aneugenic effects caused by ROS and/or the physical presence of BPA and nano-TiO_2 around the mitotic apparatus were possible reasons for increasing MN formation in L-02 cells exposed to nano-TiO_2 and BPA together.

4. Conclusion

Interactions of nano-TiO_2 with BPA increased agglomeration and zeta potential, but did not influence the adsorption capacity of nano-TiO_2. The aggregated nano-TiO_2 can enrich BPA and be uptaken into nuclei of exposed cells, which may increase intracellular BPA and nano-TiO_2 levels after L-02 cells are exposed to low levels of BPA and nano-TiO_2. Higher intracellular exposure levels contributed to the synergistic toxicity of BPA and nano-TiO_2 via increasing intracellular oxidative stress, DNA double strand breaks and chromosomal damage in L-02 cells, although nano-TiO_2 alone showed no significant cytotoxicity or genotoxicity. Only small synergic effects were observed at the concentrations of BPA and nano-TiO_2 used in this study because none of the BPA and nano-TiO_2 mixtures yielded net responses that were two fold above the additive (Tables 3–4 and Fig. S2).

Acknowledgments

This work was supported by the National Natural Science Foundation of China (Grant Nos. 30972435, 30771775 and 20728708) and by the Foundation of the State Key Laboratory of Pollution Control and Resource Reuse (Tongji University) of China (No. PCRRV10001).

Appendix A. Supplementary data

Supplementary data associated with this article can be found, in the online version, at doi:10.1016/j.jhazmat.2011.11.040.

References

[1] S. Wadhwa, C. Rea, P. O'Hare, A. Mathur, S.S. Roy, P.S.M. Dunlop, J.A. Byrne, G. Burke, B. Meenan, J.A. McLaughlin, Comparative in vitro cytotoxicity study of carbon nanotubes and titania nanostructures on human lung epithelial cells, J. Hazard. Mater. 191 (2011) 56–61.
[2] C.Y. Jin, B.S. Zhu, X.F. Wang, Q.H. Lu, Cytotoxicity of titanium dioxide nanoparticles in mouse fibroblast cells, Chem. Res. Toxicol. 21 (2008) 1871–1877.
[3] J.Y. Chen, H.J. Zhou, A.C. Santulli, S.S. Wong, Evaluating cytotoxicity and cellular uptake from the presence of variously processed TiO_2 nanostructured morphologies, Chem. Res. Toxicol. 23 (2010) 871–879.
[4] J.S. Tsuji, A.D. Maynard, P.C. Howard, J.T. James, C. Lam, D.B. Warheit, A.B. Santamariak, Research strategies for safety evaluation of nanomaterials, part IV: risk assessment of nanoparticles, Toxicol. Sci. 89 (2006) 42–50.
[5] K. Soto, K.M. Garza, L.E. Murr, Cytotoxic effects of aggregated nanomaterials, Acta Biomater. 3 (2007) 351–358.
[6] D.B. Warheit, T.R. Webb, K.L. Reed, S. Frerichs, C.M. Sayes, Pulmonary toxicity study in rats with three forms of ultrafine-TiO_2 particles: differential responses related to surface properties, Toxicology 230 (2007) 90–104.
[7] Z.E. Allouni, M.R. Cimpan, P.J. Hol, T. Skodvin, N.R. Gjerdet, Agglomeration and sedimentation of TiO_2 nanoparticles in cell culture medium, Colloids Surf. B Biointerfaces 68 (2009) 83–87.
[8] J.L. Carwile, H.T. Luu, L.S. Bassett, D.A. Driscoll, C. Yuan, J.Y. Chang, X.Y. Ye, A.M. Calafat, K.B. Michels, Polycarbonate bottle use and urinary Bisphenol A concentrations, Environ. Health Perspect. 117 (2009) 1368–1372.
[9] A. Beroniusa, C. Rudénb, H. Hakanssona, A. Hanberga, Risk to all or none? A comparative analysis of controversies in the health risk assessment of Bisphenol A, Reprod. Toxicol. 29 (2010) 132–146.
[10] B.C. Ryan, A.K. Hotchkiss, K.M. Crofton, L.E. Gray, In utero and lactational exposure to Bisphenol A, in contrast to ethinyl estradiol, does not alter sexually dimorphic behavior, puberty, fertility, and anatomy of female LE rats, Toxicol. Sci. 114 (2010) 133–148.
[11] H.A. el-Masri, K.F. Reardon, R.S. Yang, Integrated approaches for the analysis of toxicologic interactions of chemical mixtures, Crit. Rev. Toxicol. 27 (1997) 175–197.
[12] Y. Shi, J.H. Zhang, M. Jiang, L.H. Zhu, H.Q. Tang, B. Lu, Synergistic genotoxicity caused by low concentration of titanium dioxide nanoparticles and p,p′-DDT in human hepatocytes, Environ. Mol. Mutagen. 51 (2010) 192–204.
[13] K. Yang, D. Lin, B. Xing, Interactions of humic acid with nanosized inorganic oxides, Langmuir 25 (2009) 3571–3576.
[14] J.K. Jiang, G. Oberdörster, P. Biswas, Characterization of size, surface charge, and agglomeration state of nanoparticle dispersions for toxicological studies, J. Nanopart. Res. 11 (2009) 77–89.
[15] J. Wang, G. Zhou, C. Chen, H. Yu, T. Wang, Y. Ma, G. Jia, Y. Gao, B. Li, J. Sun, Y. Li, F. Jiao, Y. Zhao, Z. Chai, Acute toxicity and biodistribution of different sized titanium dioxide particles in mice after oral administration, Toxicol. Lett. 168 (2007) 176–185.
[16] E. Fabian, R. Landsiedel, L. Ma-Hock, K. Wiench, W. Wohlleben, B. van Ravenzwaay, Tissue distribution and toxicity of intravenously administered titanium dioxide nanoparticles in rats, Arch. Toxicol. 82 (2008) 151–157.
[17] A. Bouskine, M. Nebout, F. Brucker-Davis, M. Benahmed, P. Fenichel, Low doses of bisphenol A promote human seminoma cell proliferation by activating PKA and PKG via a membrane G-proteincoupled estrogen receptor, Environ. Health Perspect. 117 (2009) 1053–1058.
[18] L.E. Bennetts, G.N. De Iuliis, B. Nixon, M. Kime, K. Zelski, C.M. McVicar, S.E. Lewis, R.J. Aitk, Impact of estrogenic compounds on DNA integrity in human spermatozoa: evidence for cross-linking and redox cycling activities, Mutat. Res. 641 (2008) 1–11.
[19] E. Eruslanov, S. Kusmartsev, Identification of ROS using oxidized DCFDA and flow-cytometry, Methods Mol. Biol. 594 (2010) 57–72.
[20] K. Yagi, Simple assay for the level of total lipid peroxides in serum or plasma, Methods Mol. Biol. 108 (1998) 101–106.
[21] R.R. Tice, The single cell gel/comet assay: a microgel electrophoretic technique for the detection of DNA damage and repair in individual cells, in: D.H. Phillips, S. Venitt (Eds.), Environmental Mutagenesis, Bios Scientific Publishers, Oxford, 1995, pp. 315–339.
[22] M. Fenech, The in vitro micronucleus technique, Mutat. Res. 455 (2000) 81–95.
[23] S. Liufu, H. Xiao, Y. Li, Adsorption of poly(acrylic acid) onto the surface of titanium dioxide and the colloidal stability of aqueous suspension, J. Colloid Interface Sci. 281 (2005) 155–163.
[24] T. Xia, M. Kovochich, J. Brant, M. Hotze, J. Sempf, T. Oberley, C. Sioutas, J.I. Yeh, M.R. Wiesner, A.E. Nel, Comparison of the abilities of ambient and manufactured nanoparticles to induce cellular toxicity according to an oxidative stress paradigm, Nano Lett. 6 (2006) 1794–1807.
[25] D. Kuhnel, W. Busch, T. Meissner, A. Springer, A. Potthoff, V. Richter, M. Gelinsky, S. Scholz, K. Schirmer, Agglomeration of tungsten carbide nanoparticles in exposure medium does not prevent uptake and toxicity toward a rainbow trout gill cell line, Aquat. Toxicol. 93 (2009) 91–99.
[26] Q. Rahman, M. Lohani, E. Dopp, H. Pemsel, L. Jonas, D.G. Weiss, D. Schiffmann, Evidence that ultrafine titanium dioxide induces micronuclei and apoptosis in Syrian hamster embryo fibroblasts, Environ. Health Perspect. 110 (2002) 797–800.
[27] K.Y. Cai, Y.H. Hou, Y. Hu, L. Zhao, Z. Luo, Y.S. Shi, M. Lai, W.H. Yang, P. Liu, Correlation of the cytotoxicity of TiO_2 nanoparticles with different particle sizes on a sub-200-nm scale, Small (2011), doi:10.1002/smll.201101170.
[28] K.C. Chitra, C. Latchoumycandane, P.P. Mathur, Induction of oxidative stress by bisphenol A in the epididymal sperm of rats, Toxicology 185 (2003) 119–127.
[29] Y.J. Yang, Y.C. Hong, S.Y. Oh, M.S. Park, H. Kim, J.H. Leem, E.H. Ha, A. Bisphenol, exposure is associated with oxidative stress and inflammation in postmenopausal women, Environ. Res. 109 (2009) 797–801.
[30] E.M. Parry, J.M. Parry, C. Corso, A. Doherty, F. Haddad, T.F. Hermine, G. Johnson, M. Kayani, E. Quick, T. Warr, J. Williamson, Detection and characterization of mechanisms of action of aneugenic chemicals, Mutagenesis 17 (2002) 509–521.
[31] S. Tayama, Y. Nakagawa, K. Tayama, Genotoxic effects of environmental estrogen-like compounds in CHO-K1 cells, Mutat. Res. 649 (2008) 114–125.